The variability of high-frequency acoustic backscatter from the region near the sea surface

Peter H. Dahl and William J. Plant

Applied Physics Laboratory, College of Ocean and Fishery Sciences, University of Washington, Seattle, Washington

Final Report (Part 2 of 2) for ONR Waves in the Ocean Program
Grant No. N00014–95-1-0048

Accepted by the *Journal of the Acoustical Society of America*

January 14, 1997

REPORT DOCUMENTATION PAGE

Form Approved
OPM No. 0704-0188

1. AGENCY USE ONLY *(Leave blank)*	2. REPORT DATE	3. REPORT TYPE AND DATES COVERED
	Jan. 14, 1997	Technical

4. TITLE AND SUBTITLE
Final Report (Parts 1 and 2) for ONR Waves in the Ocean Program, Grant No. N00014-95-1-0048

5. FUNDING NUMBERS
Grant
N00014-95-1-0048

6. AUTHOR(S)
Peter H. Dahl, et al.

7. PERFORMING ORGANIZATION NAME(S) AND ADDRESS(ES)
Applied Physics Laboratory
University of Washington
1013 NE 40th Street
Seattle, WA 98105-6698

8. PERFORMING ORGANIZATION REPORT NUMBER
APL–UW

9. SPONSORING / MONITORING AGENCY NAME(S) AND ADDRESS(ES)
Dr. Jeffrey Simmen (Code 3210A)
Office of Naval Research
Ballston Tower One
800 North Quincy Street
Arlington, VA 22217-5660

10. SPONSORING / MONITORING AGENCY REPORT NUMBER

11. SUPPLEMENTARY NOTES

12a. DISTRIBUTION / AVAILABILITY STATEMENT
Unlimited.

12b. DISTRIBUTION CODE

13. ABSTRACT *(Maximum 200 words)*

Simultaneous and coincident measurements of acoustic and microwave backscatter from the air/sea interface were obtained during Phase II of the SAXON-FPN experiment in December 1992 and again in March 1993. The acoustic and microwave grazing angles were both set to 17°, and the wavelengths were matched, being set to 2.14, 3.00, and 5.66 cm, corresponding to, respectively, acoustic frequencies of 26.5, 50, and 70 kHz and microwave frequencies of 5.3, 10, and 14 GHz. The results of our experiments show that the two scattering strengths are comparable at wind speeds below about 3 m/s but that the acoustic scattering strength increases much faster than the microwave scattering strength with increasing wind speed until reaching saturation. The temporal variability of acoustic backscattering from the region near the sea surface is examined for frequencies in the 30- to 70-kHz range. A variance spectrum of the scattering strength exhibits effects associated with three different processes described in the paper.

14. SUBJECT TERMS
high-frequency, acoustic backscatter, microwave backscatter, sea surface scattering, acoustic fluctuations, sea surface spectra

15. NUMBER OF PAGES

16. PRICE CODE

17. SECURITY CLASSIFICATION OF REPORT	18. SECURITY CLASSIFICATION OF THIS PAGE	19. SECURITY CLASSIFICATION OF ABSTRACT	20. LIMITATION OF ABSTRACT
Unclassified	Unclassified	Unclassified	SAR

Abstract

The temporal variability of acoustic backscattering from the region near the sea surface is examined for frequencies in the 30- to 70-kHz range. A variance spectrum of the scattering strength exhibits effects associated with three different processes. Below about 0.1 Hz, the spectrum contains a large contribution associated with temporal variations in the advection of bubble clouds through the measurement volume by large-scale processes. At high frequencies, the spectrum asymptotes to a level characteristic of a Gaussian backscattered pressure field from randomly moving bubbles within the scattering volume. We treat the overall variability as a slow modulation of this Gaussian process by larger-scale processes and derive a probability density function for the scattering strength using Bayes' theorem. Finally, in some cases, the spectrum exhibits a peak at the frequency of the dominant surface waves. Attempts to compute coherence functions between the backscattered acoustic power and surface wave orbital velocities, measured by a microwave system observing the same spot as the acoustic system, resulted in very low values. This leads us to believe that the wave-induced peak in the acoustic backscatter variance spectrum is caused by highly nonlinear processes. A time series of acoustic backscatter from a vertically pointing system confirms the existence of this modulation at the dominant wave frequency and also suggests its nonlinear character.

I. INTRODUCTION

In a related paper (Dahl *et al.*, 1997), we demonstrated that high-frequency acoustic backscattering from the region near the sea surface is dominated by scattering from bubbles at all but very low wind speeds, for low to moderate grazing angles. Mean values of the backscattering cross section normalized by surface area were used to fit an interpretive model based on scattering from subsurface bubbles. The model adequately described the functional form of scattering vs wind speed and yielded reasonable estimates for the parameter β_I, equal to the depth-integrated extinction cross section per unit volume associated with bubbles. However, a sizable variance about the mean for a given wind speed was also observed, and here we examine this variability. In doing so we discuss measurements of both surface backscattering and volumetric backscattering from subsurface bubbles taken from two different experiments.

In the following section the two experiments from which the surface and volume scattering data originate are briefly described. In section III, variance spectra computed from time series of surface backscattering data (expressed in decibels) are discussed. The variance spectra illustrate how processes of differing time scales contribute to the total variance of surface backscattering strength. Looking ahead, we establish that the variance spectrum can be roughly partitioned into a low-frequency region (less than about 0.1 Hz) and a high-frequency region. A third region, associated with the frequencies of the dominant waves, sometimes exists. Then in section IV, a probability density function (PDF) for surface backscattering strength is developed based on partitioning the variance between low- and high-frequency fluctuations. Statistical goodness-of-fit tests confirm that the model PDF gives a good representation of the data. In section V the time scale associated with the dominant surface waves is examined in depth using the measurements of volume scattering from subsurface bubbles. It is also shown that the volume scattering data fit the same model PDF as developed in section IV.

II. EXPERIMENTAL DESCRIPTION

The data used in this paper come from two separate experiments. The first data set originates from Phase II of the Synthetic Aperture Radar and X Band Ocean Nonlinearities (SAXON)-Forshungsplatform *Nordsee* (FPN) experiment conducted in December 1991. Measurements relevant to this paper are described by Dahl *et al.* (1997). More information regarding the SAXON-FPN experimental program is given by Plant and Alpers (1994). The acoustic backscattering measurements were made by the Forschungsanstalt der Bundeswehr für Wasserschall-und Geophysik of Kiel, Germany. Here we discuss those made at a grazing angle of 17° and frequencies of 50 and 70 kHz, using two-way beamwidths of 2.9° and 2°, respectively, and a pulse width of 4 ms. The transducer depth was 24 m, and the data were sampled every 0.4 s. Backscatter data from a coherent microwave system were obtained from the same area of the sea surface simultaneously with the acoustic data, and we have utilized those from a CW K_u band (14-GHz) system for some of the results described in this paper. The half-power, two-way beamwidth of this system was 6.6° in the E plane and 5.0° in the

H plane; it was mounted 26 m above mean sea level and operated at a grazing angle of 17°.

The second data set originates from an experiment described by Dahl and Jessup (1995) that was conducted from the floating instrument platform *FLIP* in January 1992. In this case acoustic measurements of subsurface bubbles were made at vertical incidence from a 13-m-long subsurface boom attached to *FLIP*'s hull 28.5 m below the water line. The *FLIP* measurements discussed here were made at 30 kHz, using a system with a nominal two-way beamwidth of 16° and a pulse width of 1 ms, with data being sampled every 0.25 s.

III. PROCESSES CONTRIBUTING TO THE VARIANCE OF SURFACE BACKSCATTERING STRENGTH

Figure 1 shows a time series of acoustic backscatter from the sea surface that represents a continuous half-hour set of measurements made at 50 kHz. Each value is the decibel equivalent of σ_o^a, the backscattering cross-section normalized by surface area; this decibel quantity is referred to as scattering strength. The data were taken during steady wind conditions, with a mean wind speed of 5.8 m/s and a standard deviation of 0.41 m/s, giving a coefficient of variation for wind speed of around 10%. We make the assumption that this represents a single environment vis-á-vis scattering conditions. When we use the logarithmic transformation to scattering strength, $s = 10 \log_{10} \sigma_o^a$, the time series appears to have a slowly varying mean with a roughly constant additive noise component. With the variance now rather more stabilized, the time series data are more appropriate for spectral analysis than had we used linear units. Makris (1995) establishes a more complete mathematical justification for the use of logarithmic units in a variety of engineering applications, and in particular for variables that undergo fluctuations similar to σ_o^a.

Figure 2a shows estimates of the variance spectrum for the time series in Fig. 1 (thick, solid curve) and for two other scattering-strength time series made at 70 kHz during which the mean wind speed was 9.7 m/s (dashed curve) and 11.1 m/s (thin, solid curve). Figure 2b shows wave-height variance spectra from the FM part of the microwave return; we will discuss these further below. The relative wind-speed variation associated with these data was approximately the same ($\sim$ 10%) as for the data shown in Fig. 1. Note that the spectra in Fig. 2a are plotted such that the average value of the spectral function over the Nyquist bandwidth equals the total variance, and thus the ordinate is not in dB^2/Hz but rather in dB^2. We postulate that the spectral peak at $\sim$ 0.14 Hz for the higher wind-speed data is a result of a modulation caused by surface gravity waves and postpone its discussion for now.

Two features are common to all three spectra in Fig. 2a. The first is a low-frequency region corresponding to the slow variations shown in Fig. 1. This region is very similar in spectral slope (the spectra fall between 1 and 2 orders of magnitude in the decade 0.01 to 0.10 Hz) and bandwidth ($\sim$ 0.1 Hz) to the spectra for low-frequency variation in bubble-mediated sound speed reported by Lamarre and Melville (1994), who attribute this variation to the passage of bubble clouds over their instrument. There is recent speculation (Thorpe,

1992, and Melville *et al.*, 1995) that such low-frequency variation is associated with the group frequencies of surface waves. In any case, we would expect a similar variation caused by the passage of bubble clouds under the surface scattering patch and through the effective scattering volume for the acoustic measurements discussed here. Note that the spectral averaging in Fig. 2a was carried out using 256-point FFTs with a Hanning window and 50% overlap; analysis using longer processing windows shows that the spectral density continues to increase with decreasing frequency for frequencies < 0.01 Hz (though at diminished rate), reaching a broad peak at approximately 0.005 Hz.

The second feature is the spectrum baseline level of approximately 5.57^2 (dotted line), a value equal to the variance of a random variable expressed in decibels, whose probability density function (PDF) for the linear form of the variable is exponential (Dyer, 1970; Dahl and Mathisen, 1983). The implication in our case is that the exponential PDF is a good model for fluctuations in σ_o^a, provided the time scale over which these fluctuations are observed is kept short enough. It is reasonable to assume that each observation of σ_o^a separated by 0.4 s is an independent random variable. Thus, away from the low-frequency variation, the time series data represent a white-noise, or *purely random*, process (e.g., see Percival and Walden, 1993). Note, however, that if the observations are spaced too closely in time they will eventually become correlated. Here the relevant correlation time scale, τ, is the period over which the phase of the complex scattered amplitude has changed by $\pi/2$ owing to random motion within the assembly of bubbles. For example, at 50 kHz the wavelength is 3 cm, and we would expect decorrelation in time when $|v|\tau \approx 0.0075$ cm, where $|v|$ is the characteristic speed of bubble motion, which is largely determined by the orbital motion due to gravity waves. We estimate τ is $O(10)$ ms. The exponential PDF arises naturally in many high-frequency acoustic applications where the observed scatter is the vector sum of several randomly phased scattering sources, as would occur in scattering from a random assemblage of bubbles. Were nothing to change other than the random movement of bubbles, the result would be a Gaussian backscattered pressure field with an amplitude following a Rayleigh PDF and its square, or intensity, following an exponential PDF.

IV. THE PROBABILITY DENSITY FUNCTION AND VARIANCE OF SURFACE BACKSCATTERING STRENGTH

The bandwidth of approximately 0.1 Hz roughly bounding the low-frequency, high-energy region of the spectra in Fig. 2a points to an integral time scale, T, of $O(10)$ s with which to average out the higher-frequency fluctuations. We thus compute a linear average of σ_o^a defined as $\lambda = \langle \sigma_o^a \rangle_T$, where T equals 10 s, or 25 realizations of σ_o^a based on the 0.4-s ping cycle. A histogram (Fig. 3) of $10 \log_{10} \lambda$ for the data in Fig. 1 is reasonably well approximated by a Gaussian curve with a mean, μ_T, equal to -30.63 dB and a standard deviation, σ_T, equal to 3.07 dB. This suggests that λ, the slowly varying mean value of σ_o^a, is distributed lognormally, with a PDF equal to

$$p_\lambda(\lambda) = \frac{e^{-(\log \lambda - \mu_1)^2/(2\sigma_1^2)}}{\lambda \sigma_1 \sqrt{2\pi}}, \tag{1}$$

where $\sigma_1 = \sigma_T/k$, $\mu_1 = \mu_T/k$, and $k = 10\log_{10} e$. For reference, we note that the expected value of λ is given by

$$E(\lambda) = e^{\mu_1 + \sigma_1^2/2}. \tag{2}$$

One would use Eq. (2) to relate estimates of μ_T and σ_T back to $\langle \sigma_o^a \rangle_{T^\star}$, where $T^\star$ is the total length of time over which measurements of σ_o^a were made and during which the environment is viewed as essentially unchanged. Thus, for example, theoretical estimates based on linear ensemble averages would relate to $E(\lambda)$.

Next, we take an approach analogous to that taken by Gotwols and Thompson (1994) in their statistical modeling of microwave backscattering data. Our approach differs from theirs in that we choose to work in decibels or log-transformed variables (as in the spectral estimates). Specifically, we model the PDF $p_s(s)$ for the data in Fig. 1 as an instantaneous PDF $p_{s|\lambda}(s \mid \lambda)$ governed by a slowly varying mean whose PDF is $p_\lambda(\lambda)$. To remove the condition on λ we multiply by the density for λ and integrate (Bayes' theorem), giving

$$p_s(s) = \int_0^\infty p_{s|\lambda}(s\,|\,\lambda) p_\lambda(\lambda)\, d\lambda\,, \tag{3}$$

where $p_\lambda(\lambda)$ is Eq.(1) and the conditional PDF is

$$p_{s|\lambda}(s\,|\,\lambda) = \frac{e^{-e^{s/k}/\lambda + s/k}}{k\lambda}. \tag{4}$$

Equation (4) represents a PDF that has been used to study decibel quantities such as acoustic transmission loss (Dyer, 1970; Frisk, 1978) or acoustic scattering from fish (Dahl and Mathisen, 1983), where λ (now used as a parameter) is either equal, or proportional, to mean intensity, and where variation in the linear intensity variable is described by an exponential PDF.

Equation (3) is evaluated numerically, and the results for the PDF $p(s)$ (Fig 4a) and its cumulative distribution function (CDF) counterpart (Fig. 4b) are shown compared with the data from Fig. 1. Both forms give a good representation of the data, with, as expected, the integrated form looking better. A chi-square (χ^2) goodness-of-fit test (Sachs, 1984) comparing observed with expected relative frequencies was carried out to assess the hypothesis that the data in Fig. 1 are distributed according to (3) when using sample parameters μ_1 and σ_1. The probability of the χ^2 statistic was 0.20, indicating that (3) is indeed an adequate statistical model for the data.

The first two moments of $p(s)$ are evaluated via

$$E(s^n) = \int_0^\infty \int_{-\infty}^\infty s^n p_{s|\lambda}(s \mid \lambda) ds \;\; p_\lambda(\lambda) d\lambda\,, \tag{5}$$

giving

$$E(s) = \mu_T - C_E k, \tag{6}$$

where C_E is Euler's constant (0.577215...), with the variance given by

$$\mathrm{Var}(s) = \frac{k^2\pi^2}{6} + \sigma_T^2. \tag{7}$$

Thus the effect of the slow variation is simply to add σ_T^2 to an underlying variance of 5.57^2. The standard deviation of the time series in Fig. 1, for example, is 6.42 dB, a value well approximated by $\sqrt{\sigma_T^2 + 5.57^2}$ when using the sample standard deviation for the slowly varying mean of 3.07 dB.

V. LONG WAVE MODULATION

We now return to the peak at ~ 0.14 Hz seen in the variance spectrum of the acoustic data taken at the higher wind speed (thin, solid curve in Fig. 2a). Figure 2b shows three surface wave-height spectral densities obtained from the microwave Doppler shifts. This is a standard technique for measuring wave spectra (Plant *et al.*, 1983), though typically applied for grazing angles near 45°; at 17° grazing angle, the total wave-height variance is not completely recovered for reasons discussed elsewhere (Plant, 1996). In any case, our main purpose for presenting these spectra is to show information on the dominant wave frequency, so we have normalized the spectral densities to the peak value of the highest density. The peak frequency (when resolved) and significant wave heights are noted for each case; the wave-height estimates correspond in time but were obtained from a nearby wave buoy. With the exception of the lower-wind-speed case, these wave-height spectra correspond precisely in time, and space, to the variance spectra shown in Fig. 2a. In the lower-wind-speed case, the wave-height spectrum was obtained at the same location but during the hour immediately following the acoustic measurements (hence the small difference in wind speed); the significant wave height measured by the wave buoy did not change over the 2-hour period.

Referring to the wave-height spectra, the peak frequency in the data taken at a wind speed of 11.1 m/s matches the peak in the acoustic variance spectrum in Fig. 2a, whereas the peak frequency in the data taken at 9.7 m/s has no acoustic counterpart. Likewise, only a small, broad peak is seen in the wave spectrum obtained at 6.0 m/s, and none is seen in the acoustic data. The frequency coherence between the time series of acoustic backscattering strengths and the microwave Doppler offset (proportional to wave orbital velocity) was < 0.2 for frequencies in the range of the dominant surface waves. This low coherence leads us to postulate that the peak in the acoustic variance spectrum is caused by a process that is related to the dominant surface waves but that is highly nonlinear. The nonlinearity would also explain why clearly resolvable peaks in the wave spectra as measured by the radar show an acoustic counterpart only for large-amplitude waves. At this stage we can only speculate as to the nature of the source of acoustic modulation near the dominant wave frequency. One possibility might be microscale breaking occurring preferentially on wave crests; another is discussed below in the context of FLIP data. Beam-pattern effects may also be in part responsible for the observed modulation.

In contrast to the SAXON-FPN data, where measurements of surface scattering are interpreted in terms of volume scattering from near-surface bubbles, the *FLIP* data represent unambiguous volume scattering from near-surface bubbles. We therefore studied the variability seen in this data set to obtain further insight into the variability observed in the surface-scattering data from SAXON-FPN. Figure 5a shows the variance spectrum for a

20-min time series of acoustic volume backscattering made at vertical incidence from *FLIP* during which the mean wind speed was 9.8 m/s. In this case, each value of the original time series is $s = 10 \log_{10} s_V$, where s_V is the backscattering cross section per unit volume for a given ping cycle. (The decibel quantity here will be referred to as volume backscattering strength.) The scattering center for s_V is 1 m below the time-varying surface elevation determined by the two-way acoustic travel time for the surface return.

The variance spectrum for the volume-backscattering-strength measurements from *FLIP* is remarkably similar to the spectra for the surface-backscattering-strength measurements from SAXON-FPN shown in Fig. 2a, insofar as having a high-energy region for low frequencies ($f \lesssim 0.1$ Hz) and coming close to the theoretical background limit of 5.57^2 for higher frequencies out to the Nyquist limit, which in this case extends to 2 Hz. (Figure 5a is plotted in the manner of Fig. 2a to account for the difference in Nyquist interval.) There is a peak within the low-frequency region near 0.07 Hz, and we postulate that this, too, is associated with the dominant surface waves.

Lamarre and Melville (1994) also discuss a peak in their sound speed anomaly spectra associated with the spectral peak of the dominant waves, in the context of orbital motion of these dominant waves. An alternative (though closely related) explanation is as follows: Firstly, the inhomogeneous, or patchy, bubble field lateral structure is periodically displaced to and fro a distance of order $2A$, where A is amplitude of the dominant surface waves. We would expect to see a signal in the variance spectrum of acoustic measurements at dominant wave frequencies, once $2A$ reaches or exceeds some integral horizontal scale of these patches. To be sure, however, much remains to be learned about the wave-number spectrum of the bubble field near the ocean surface. A starting point should include Gilbert (1993), who discusses this wave-number spectrum in the context of low-frequency acoustic backscatter, and Thorpe (1992). Secondly, the bubble field is periodically *distorted* while undergoing displacement by the surface wave orbital velocities, which may also add to the acoustic variation observed.

Figure 5b shows the wave-height spectrum as determined by the acoustic-travel-time data and normalized by its peak value. As in the spectra derived from the radar measurements, those derived from the acoustic travel time are simultaneous, colocated, and noninvasive with respect to the scattering. The 3-dB surface footprint of the sonar (diameter ~ 8 m) sets the high-frequency spectral cutoff for this method at approximately 0.4 Hz. However, this has little effect on the total wave-height variance, which was dominated by swell, and wave-height spectra derived in this manner agree well with those derived from measurements by a wire wave gauge and a radar altimeter which operated on the opposite side of *FLIP*. The dominant peak in the wave-height spectrum at 0.07 Hz (Fig. 5b) is roughly aligned with a broad peak in the variance spectrum (Fig. 5a). Again, however, the modulation is a nonlinear one, as the frequency coherence between the time series of wave height and $10 \log_{10} s_V$ is < 0.2 for all frequencies.

This kind of modulation, linked to both wave oribital velocity and the bubble field, would also be in effect for the SAXON-FPN data, for which we have argued that bubbles are the primary source of backscatter. It is tempting to associate this modulation with the

large peak at 0.14 Hz in Fig. 2a. The geometry of the SAXON-FPN experiment, however, also requires that we allow for the possibility of effects due simply to the variable location of the air/sea interface in the ensonified volume. The modulation observed at these low grazing angles, therefore, may well result from a combination of bubble-field modulation and purely geometric effects.

Before leaving this topic, we briefly mention two other cases in which acoustic measurements of bubbles show fluctuations related to the surface wave spectrum. Medwin *et al.* (1975) measured sound phase fluctuations near the sea surface and showed that small changes in water pressure (due to surface wave action) at the depth of the measurement probe can modulate the resonance frequency of bubbles and therefore their phase measurements. This change in resonance frequency as a function of pressure can be linearized, and a high coherence was observed between sound phase fluctuations and surface wave height at the dominant wave frequencies. This mechanism is less applicable to the FLIP data because these measurements were effectively wave-following, and so crest-to-trough pressure difference is no longer a first-order quantity. Zedel and Farmer (1994) observed a modulation in ambient sound level that was in phase with surface displacement directly above their measurement probe. A number of potential source mechanisms were identified, including small-scale wave-breaking events triggered by long-wave/short-wave interaction. Again, however, as in the observations by Medwin *et al.*, there was high coherence between fluctuations in noise level and surface wave height, which we do not see in our data. Thus the picture remains unclear, and we will seek to clarify the role of wave modulation in future studies.

Finally, it is useful to view the portion of the variance spectra above the dotted line in Figs. 2a and 5a as variability in excess of the theoretical 5.57^2. Let us define the low-frequency excess as the portion above the dotted line for $f < 0.1$ Hz. This component makes up roughly 20–30% of the total variance for the SAXON-FPN data (Fig. 2a) and about 40% of the total variance for the *FLIP* data (Fig. 5a). The component due to wave modulation in Fig. 2a, between approximately 0.1 and 0.3 Hz, comprises about 10% of the total variance. For the *FLIP* data, wave modulation is, in part, added to the low-frequency region as we have defined it, with the region between 0.1 and 0.2 Hz contributing less than 10% to the total variance.

Following the procedure used earlier with the backscattering data, we compute a linear average of the *FLIP* data, defined in this case as $\lambda = \langle s_V \rangle_T$, where we again use an averaging time scale, T, equal to 10 s, giving $\mu_T = -50.7$ dB and $\sigma_T = 3.4$ dB to use in Eqs. (2) and (3). The results are shown in Fig. 6. The probability of the χ^2 statistic is 0.25, which suggests that our PDF model applies equally well to the s_V measure.

In general, the variance spectrum provides guidance as to the choice of T. In the *FLIP* data (Fig. 5a), for example, 0.1 Hz roughly defines the point at which the excess variability is confined to lower frequencies, and thus $T = 10$ s should be appropriate, as confirmed in Fig. 6 and the reasonably probable value for the χ^2 statistic. On the other hand, the variance spectrum for the SAXON-FPN data taken at 11.1 m/s (thin, solid curve in Fig. 2a), with its large and isolated peak, points to an averaging time scale of 3 s, because ~ 0.3 Hz now

roughly defines the point at which the excess variability is confined to lower frequencies. If we, in fact, use $T = 10$ s for these data, we find $\mu_T = -29.59$ dB and $\sigma_T = 3.88$ dB, giving a rather a low probability (< 0.01) for the χ^2 goodness-of-fit parameter. Using these values for μ_T and σ_T, we would reject the hypothesis (at the 5% level of significance) that the data are distributed according to our PDF model. But if we use $T = 3$ s, then μ_T lowers somewhat to -30.06 dB and σ_T increases to 4.41 dB, with the probability of the χ^2 statistic improving to 0.05. This probability is less than in the two earlier trials but sufficiently high that the hypothesis is not rejected.

The results for both T values are shown in Fig. 7. The model/data agreement is better with $T = 3$ s (dashed curve), although using $T = 10$ s (bold, solid curve) still captures the essential features of the empirical PDF (Fig. 7a) and CDF (Fig. 7b). Thus, notwithstanding the existence of peaks in the variance spectra associated with the dominant surface waves, an averaging time scale of 10 s seems to be remarkably robust. Accordingly, we examined σ_T, for $T = 10$ s, for the entire SAXON-FPN Phase II data set spanning 4 days (and including data taken at the third frequency of 26.5 kHz). Contiguous segments of data were defined by having the coefficient of variation for wind speed remain $< 10\%$, following our definition of an unchanging environment, with typical segment lengths (such as the one shown in Fig. 1) equaling 30 min. The result, for wind speeds between 3.8 and 11.6 m/s, can be summarized by $\sigma_T \approx -0.18U_{10} + 4.85$, in decibels, where U_{10} is wind speed corrected to 10-m height. The reduction in variance as wind speed increases is consistent with a less patchy bubble field at higher wind speeds and with saturation (e.g., see Dahl *et al.*, 1997), which places an upper bound on the scattering and thereby reduces the variance.

VI. SUMMARY AND CONCLUSION

We have studied fluctuations in measurements of acoustic backscattering from the sea surface made during the SAXON-FPN experiment, for which the mean values are shown in another paper to be linked to the concentration of near-surface bubbles. For comparison, our study also included the fluctuations in volumetric backscattering from near-surface bubbles, using data gathered from *FLIP*. Spectral analysis was carried out on the equivalent decibel form for the data from each experiment, and three features in the variance spectrum were identified. At low frequencies, $f \lesssim 0.1$ Hz, we suggest that the variability is caused by bubble clouds being advected through the ensonified region; the spectral roll-off in this region was found to be between f^{-1} and f^{-2}. At the frequencies of the dominant surface waves, a modulation is induced if the wave height is sufficiently large, and we suggest, based on the low coherence of this modulation with the dominant waves, that it may be highly nonlinear. The *FLIP* data showed consistency with this modulation being linked to the action of the dominant surface waves. Finally, at high frequencies, the backscattered pressure field is Gaussian, as expected for scattering from a large number of independent scatterers. The standard deviation of this part of the scatter, on a logarithmic scale, is 5.57 dB.

Decibel quantities were used in our analysis to stabilize the variance and to allow comparison of the fluctuations in acoustic measures, such as σ_o^a and s_V, that differ in both

dimension and nominal value but otherwise are proportional to backscattered intensity. We modeled the PDF for a decibel quantity, e.g., scattering strength, as the integral over the product of an instantaneous PDF, which corresponds to an exponential PDF for the quantity in linear space conditioned on a value λ, the normalized cross section averaged over a time T, and the PDF for λ. The λ value undergoes low-frequency modulation, and we model its PDF as lognormal. This model reproduces the data well and indicates that the total variance of the scattering strength is simply 5.57^2 plus the variance of the low-frequency modulation, σ_T^2. A representative estimate of σ_T (for $T = 10$ s) for the entire SAXON-FPN Phase II data set taken at a grazing angle of 17° is approximately 3.7 dB.

ACKNOWLEDGMENTS

This study was supported by the Office of Naval Research through grant N00014-95-1-0048 from the Ocean Acoustics Program. Constructive comments by an anonymous reviewer are much appreciated.

REFERENCES

Dahl, P. H., and Mathisen, O. A. (**1983**). "Measurement of fish target strength and associated directivity at high frequencies," J. Acoust. Soc. Am. **73**, 1205–1211.

Dahl, P. H., and Jessup, A. T. (**1995**.) "On bubble clouds produced by breaking waves: An event analysis of ocean acoustic measurements," J. Geophys. Res. **100**, 5007–5020.

Dahl, P. H., Plant, W. J., Nützel, B., Schmidt, A., Herwig, H., and Terray, E. A. (**1997**). "Simultaneous acoustic and microwave backscattering from the sea surface," J. Acoust. Soc. Am., this issue.

Dyer, I., (**1970**). "Statistics of sound propagation in the ocean," J. Acoust. Soc. Am. **48**, 337–345.

Frisk, G. V. (**1978**). "Intensity statistics for long-range acoustic propagation in the ocean," J. Acoust. Soc. Am. **64**, 257–259.

Gilbert, K. E., (**1993**). "A stochastic model for scattering from the near-surface oceanic bubble layer," J. Acoust. Soc. Am. **94**, 3325–3344.

Gotwols, B. L., and Thompson, D. R. (**1994**). "Ocean microwave backscatter distributions," Geophys. Res. **99**, 9741–9750.

Lamarre, E., and Melville, W. K. (**1994**). "Sound-speed measurements near the ocean," J. Acoust. Soc. Am. **96**, 3605–3616.

Makris, N.C., (**1995**). "A foundation for logarithmic measures of fluctuating intensity in pattern recognition," Opt. Lett. **20**, 2012–2014.

Medwin, H., Fitzgerald, J., and Rautmann, G. (**1975**). "Acoustic miniprobing for ocean microstructure and bubbles," J. Geophys. Res. **80**, 405–413.

Melville, W. K., Terrell, E., and Ding, L. (**1995**). "Field measurements of air entrainment by breaking waves," in *Air–Water Gas Transfer: Selected Papers from the Third International Symposium on Air–Water Gas Transfer*, edited by B. Jähne and E. C. Monahan (AEON Verlag & Studio, Hanau), pp. 286–295.

Percival, D. B., and Walden, A.T. (**1993**). *Spectral Analysis for Physical Applications: Multitaper and Conventional Univariate Techniques* (Cambridge University Press, Cambridge, U.K.).

Plant, W. J. (**1996**). "A model for microwave Doppler sea return at high incidence angles: Bragg scattering from bound, tilted waves," submitted to J. Geophys. Res.

Plant, W. J., Keller, W. C., and Cross, A. (**1983**). "Parametric dependence of ocean wave–radar modulation transfer functions," J. Geophys. Res. **88**, 9747–9756.

Plant, W. J., and Alpers, W. (**1994**). "An introduction to SAXON-FPN," J. Geophys. Res. **99**, 9699–9703.

Sachs, L. (**1984**). *Applied Statistics: A Handbook of Techniques* (Springer-Verlag, New York).

Thorpe, S. A. (**1992**). "Bubble clouds and the dynamics of the upper ocean," Q. J. Meteorol. Soc. **118**, 1–22.

Zedel, L., and Farmer, D. (**1994**). "Surface wave period modulations in near surface ambient sound," J. Geophys. Res. **99**, 8041–8052.

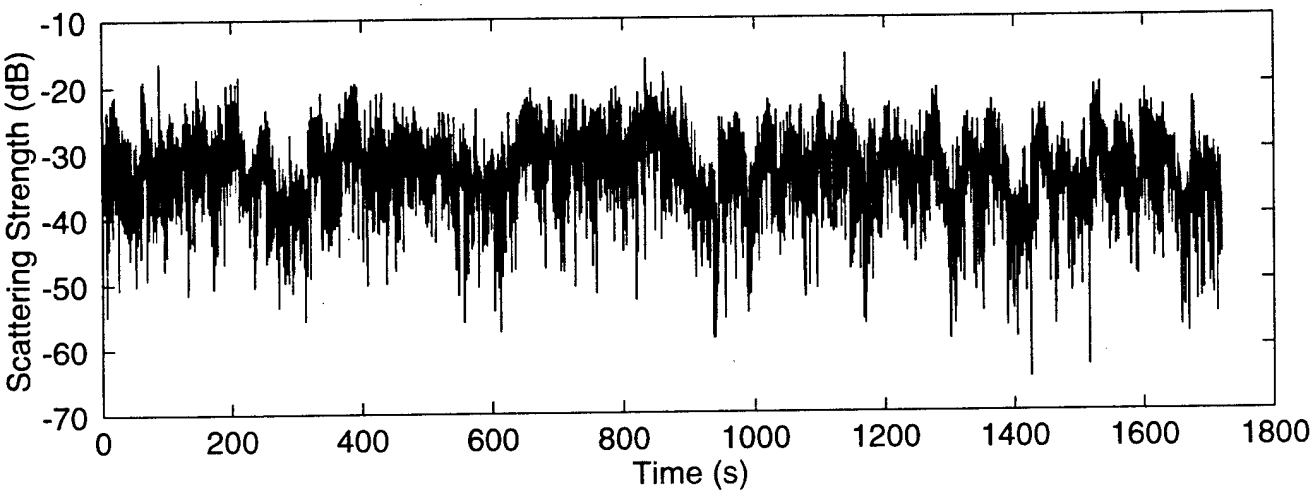

FIG. 1. Time series of 50-kHz acoustic scattering strength at a 17° grazing angle. The wind speed was 5.8 m/s at the time of data collection, 1616 UTC on December 3, 1991.

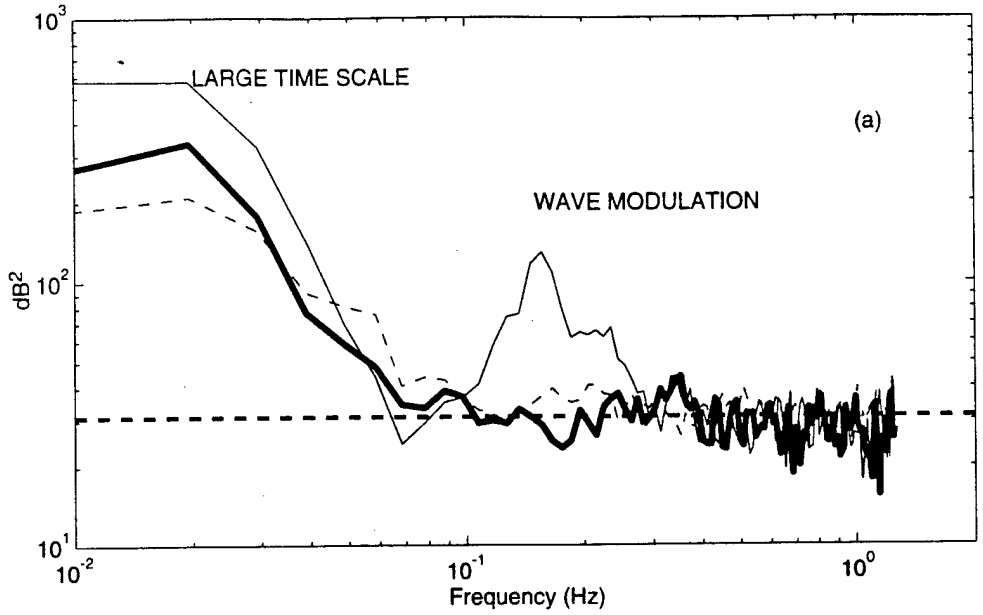

FIG. 2a. Variance spectra for the data shown in Fig. 1 (thick bold curve) and for other times series of acoustic scattering strength made at 70 kHz during which the mean wind speed was 9.7 m/s (dashed curve) and 11.1 m/s (thin, solid curve). The dotted line equals the theoretical spectrum baseline value of 5.57^2 dB^2.

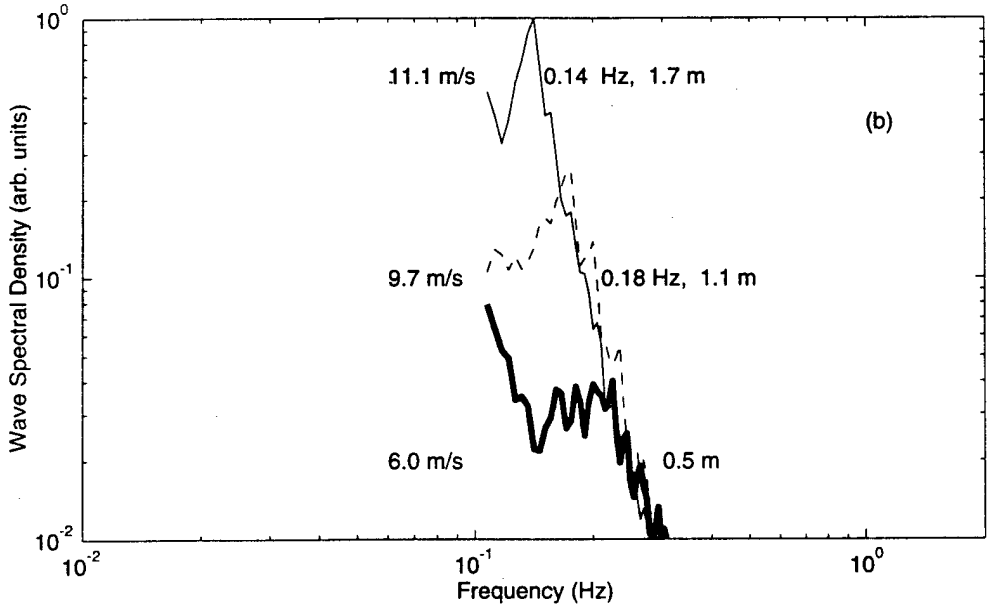

FIG. 2b. Surface wave-height spectra derived from K_u-band Doppler offset. All spectra are normalized by the peak value of the spectrum taken at a wind speed of 11.1 m/s. The line types correspond to those in Fig. 2a; to the right of each spectrum is an estimate of the peak wave frequency and significant wave height (with the exception of the bold curve, where the peak in the spectrum is very broad).

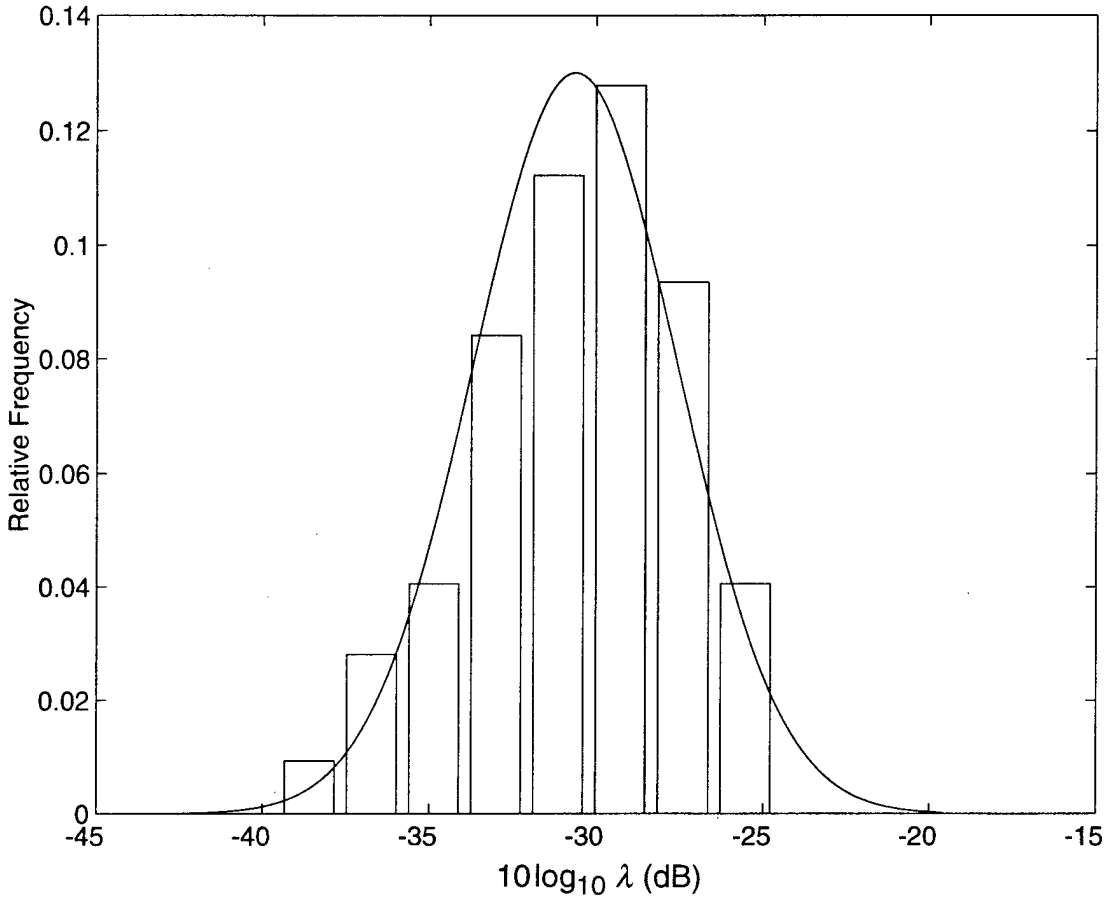

FIG. 3. Histogram of $10\log_{10}\lambda$ for the data of Fig. 1. Here, λ is the linear mean of σ_o^a over 10 s. The curve represents a Gaussian probability density function with a mean equal to -30.63 dB and a standard deviation equal to 3.07 dB.

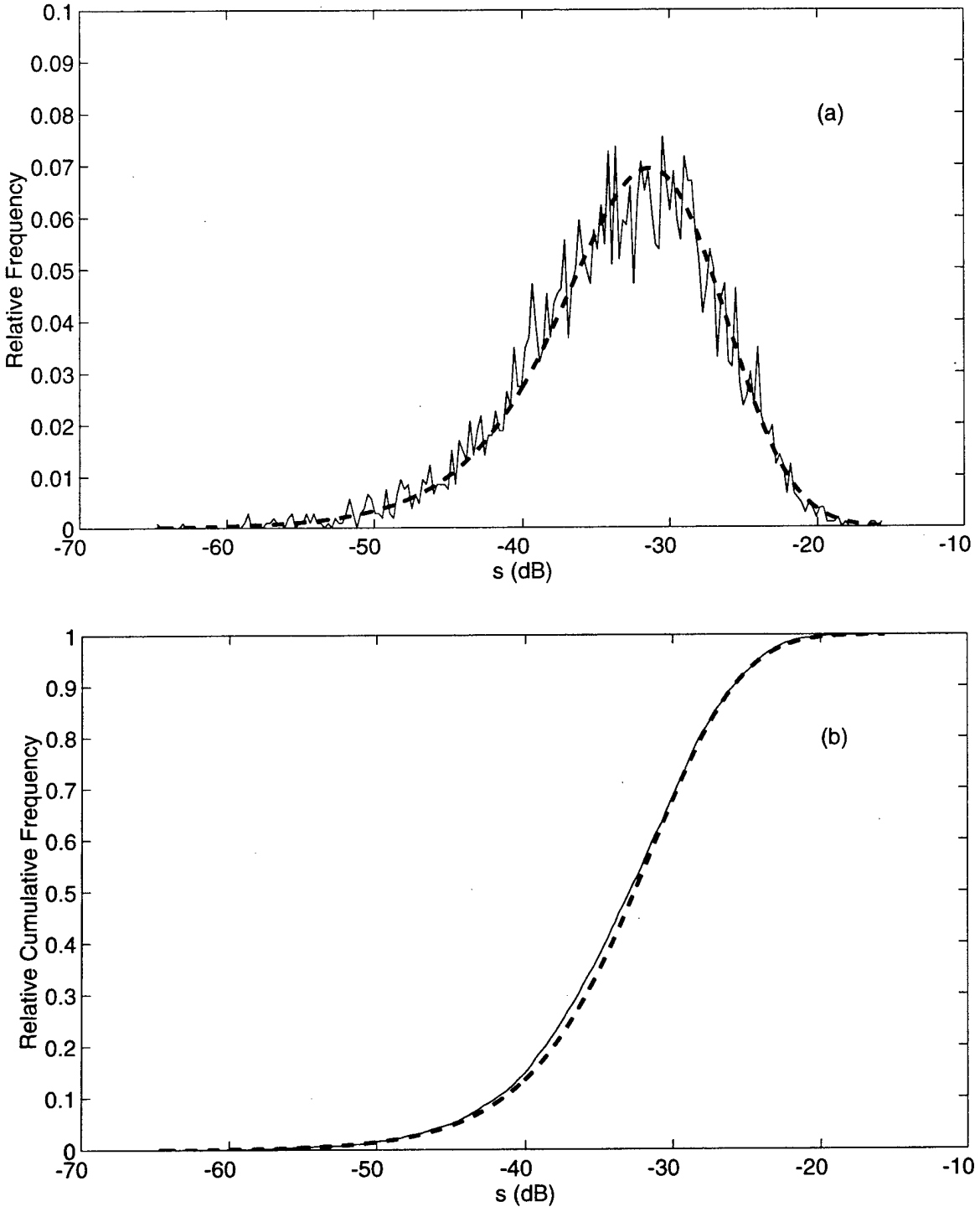

FIG. 4. Probability density function (a) and cumulative distribution function (b) for the SAXON-FPN data of Fig. 1 (thin, solid curves) taken at a wind speed of 5.8 m/s compared with model predictions (dashed curves). The model is computed from Eqs. (1), (3), and (4), using $\mu_T = -30.63$ dB and $\sigma_T = 3.07$ dB. The probability of the χ^2 statistic is 0.20.

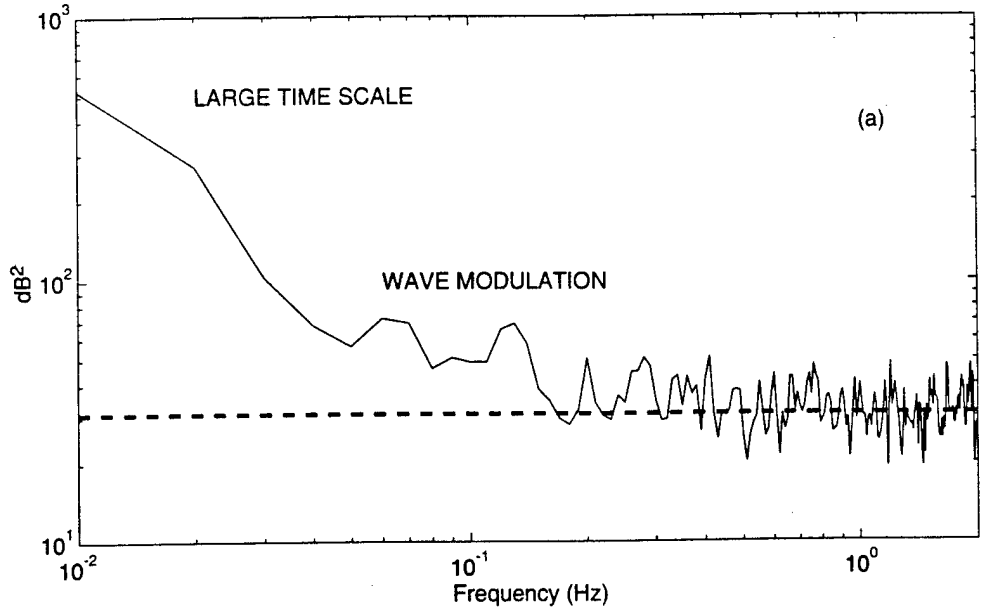

FIG. 5a. Variance spectrum of volume backscattering strength measured at vertical incidence from the research platform *FLIP*. The mean wind speed was 9.8 m/s. The dotted line equals the theoretical spectrum baseline value of 5.57^2 dB^2.

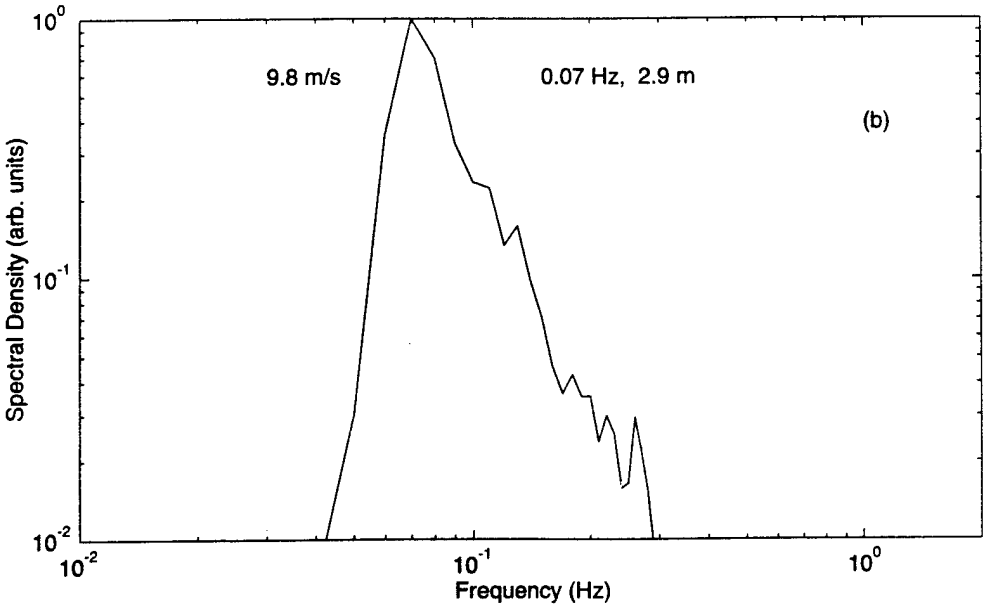

FIG. 5b. Surface wave-height spectrum derived from acoustic travel time, for times corresponding to the data shown in Fig. 5a. The spectrum is normalized to its peak value with peak wave frequency and significant wave height noted on the right.

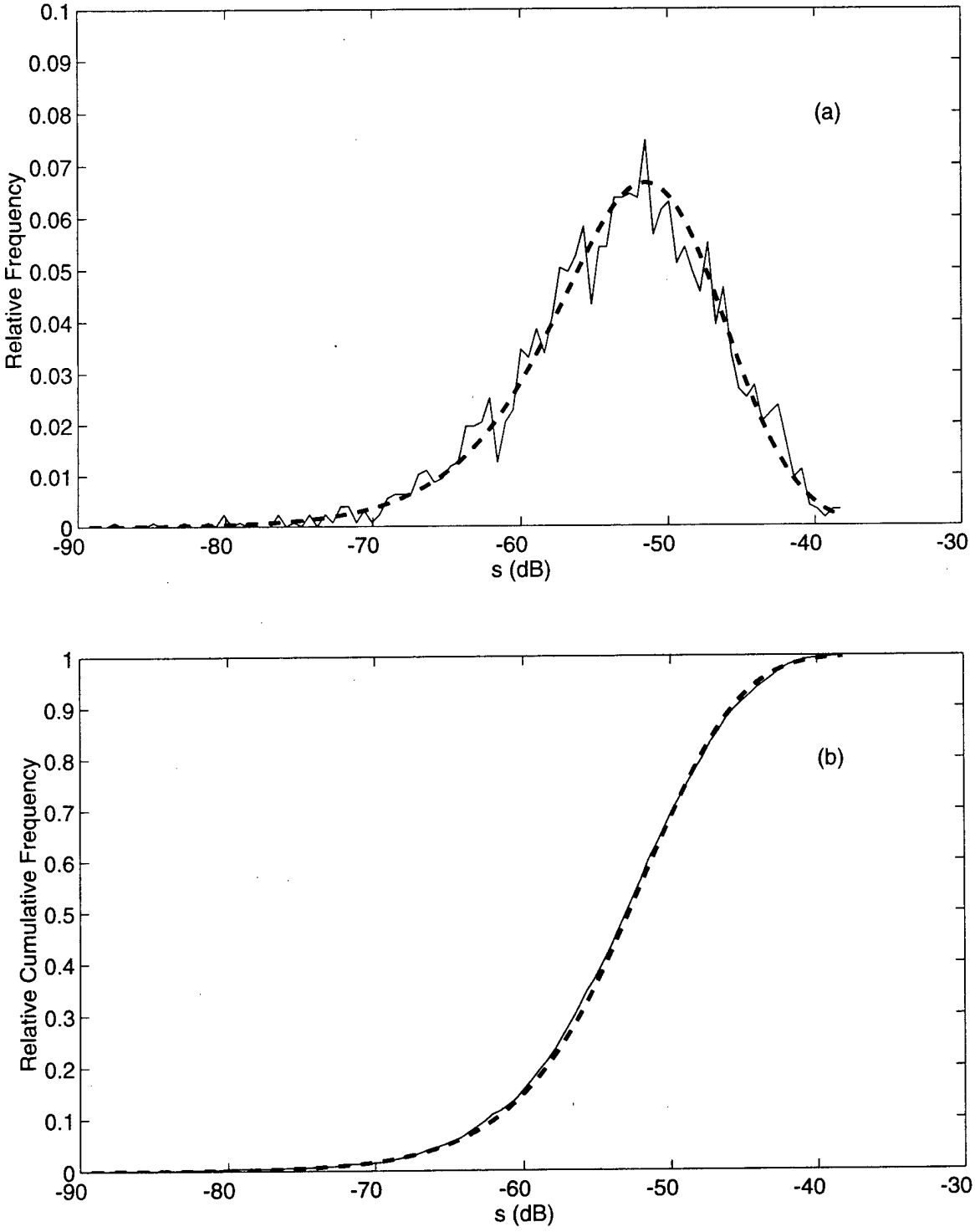

FIG. 6. Probability density function (a) and cumulative distribution function (b) for the *FLIP* data in Fig. 5 (thin, solid curves) taken at a wind speed of 9.8 m/s compared with model predictions (dashed curves). The model is computed from Eqs. (1), (3), and (4), using $\mu_T = -50.67$ dB and $\sigma_T = 3.45$ dB. The probability of the χ^2 statistic is 0.25.

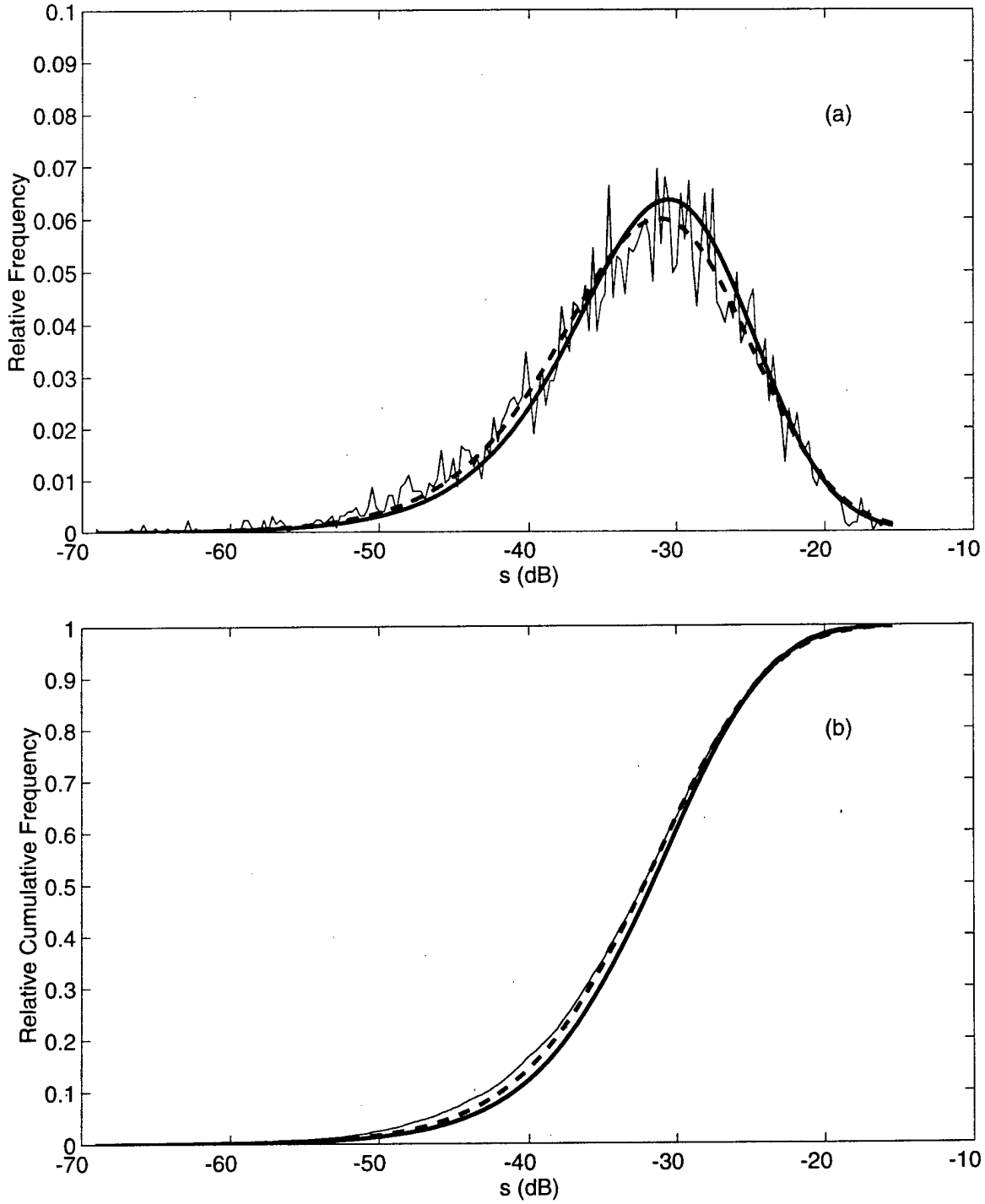

FIG. 7. Probability density function (a) and cumulative distribution function (b) for the SAXON-FPN data (thin, solid curves) taken at a wind speed of 11.1 m/s compared with model predictions. The model is computed from Eqs. (1), (3), and (4). The probability of the χ^2 statistic is < 0.01 when using $\mu_T = -29.59$ dB and $\sigma_T = 3.88$ dB, based on $T = 10$ s (thick, solid curve). The probability of the χ^2 statistic is 0.05 when using $\mu_T = -30.06$ dB and $\sigma_T = 4.41$ dB, based on $T = 3$ s (dashed curve).